

Electronic Supplementary Information (ESI) for Materials Chemistry Frontiers

Cationic covalent organic framework based all-solid-state electrolytes

Zhen Li,^{a,b} Zhi-Wei Liu,^{b,c} Zhen-Jie Mu,^b Chen Cao,^a Zeyu Li,^a Tian-Xiong Wang,^{b,d} Yu Li,^a Xuesong Ding,^{b,*} Bao-Hang Han,^{b,d,*} Wei Feng^{a,e,*}

^a *School of Materials Science and Engineering, Tianjin University, Tianjin 300072, China*

^b *CAS Key Laboratory of Nanosystem and Hierarchical Fabrication, CAS Center for Excellence in Nanoscience, National Center for Nanoscience and Technology, Beijing 100190, China*

^c *Sino-Danish Center for Education and Research, Sino-Danish College, University of Chinese Academy of Sciences, Beijing 100190, China*

^d *University of Chinese Academy of Science, Beijing 100049, China*

^e *Collaborative Innovation Center of Chemical Science and Engineering, Tianjin 300072, China*

Materials

Tetrahydrofuran (THF), 1,4-dioxane, methanol, mesitylene, hydrochloric acid, toluene, chloroform, *N,N*-dimethylformamide (DMF), *N*-methyl pyrrolidone (NMP) and other commonly used organic solvents were purchased from Sinopharm Chemical Reagent Co. Potassium carbonate (K_2CO_3), copper sulfate ($CuSO_4$), 4-(bromomethyl)benzonitrile, 1,3,5-tris(4-formyl-phenyl)benzene (TFPB), 1,3,5-tribromobenzene, imidazole, diisobutyl aluminium hydride (DIBAl-H), benzidine (BZ), 4-aminobiphenyle (4-AB), lithium iron phosphate ($LiFePO_4$), Super P, poly(vinylidene fluoride) (PVDF), and lithium bis(trifluoromethane) sulfonimide (LiTFSI) were purchased from Energy Chemical Co. All chemicals and solvents were reagent grade and used without further purification, unless with particularly noted.

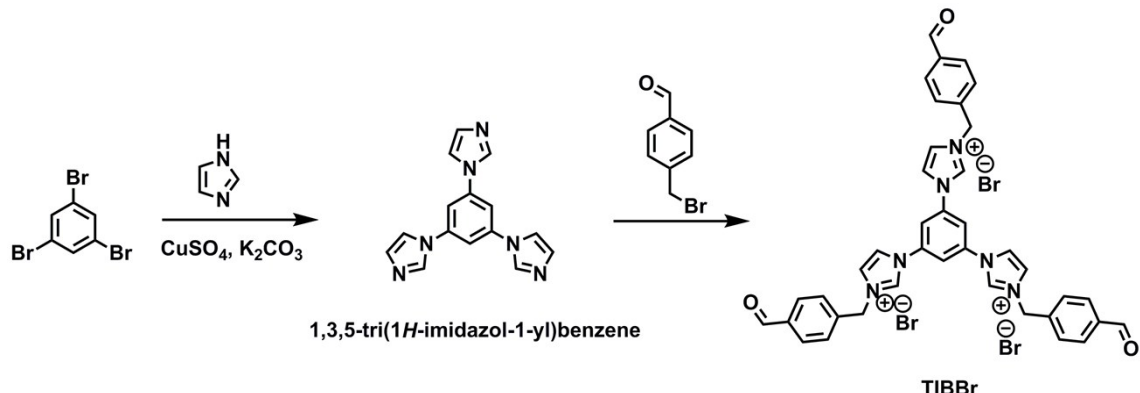
Instrumental characterization

The 1H and ^{13}C NMR spectra were recorded on a Bruker DMX-400 NMR spectrometer (Bruker, Germany) with tetra-methylsilane (TMS) as an internal reference. Powder X-ray diffraction (PXRD) patterns were measured by Xeuss SAXS/WAXS system (Xenocs, France) with Cu K α radiation ($\lambda = 1.5418 \text{ \AA}$). Molecular modeling and Pawley refinement were carried out using Reflex, a software package for crystal determination from PXRD pattern, implemented in Material Studios 2017/R2 modeling (Accelrys Inc.). Unit cell dimension was first manually determined from the observed PXRD peak positions using the coordinates. The Pawley refinement was performed to optimize the lattice parameters iteratively until the R_{WP} value converges. The refinement

indicates a triclinic crystal system with a unit cell of $a = 59.33 \text{ \AA}$, $b = 60.02 \text{ \AA}$, $c = 3.56 \text{ \AA}$, $\alpha = 91.17^\circ$, $\beta = 89.80^\circ$, and $\gamma = 118.94^\circ$. The pseudo-Voigt profile function was used for whole profile fitting and Rietveld function was used for asymmetry correction during the refinement processes. The final R_{WP} and R_{P} values were 9.78 and 4.67% for Im-COF-Br. Simulated PXRD patterns were calculated for (1) an eclipsed AA-stacking of $P1$ space group, and (2) a staggered stacking of $P1$ space group. The Fourier transform infrared spectroscopy (FT-IR) spectra were recorded on Spectrum One (Perkin-Elmer Instruments Co. Ltd, USA). Solid-state ^{13}C cross-polarization magic angle spinning (CP/MAS) NMR data were derived from Bruker Advance III 400 spectrometer (Bruker, Germany). Thermogravimetric analyses (TGA) were performed using a Pyris Diamond thermogravimetric/differential thermal analyzer (Perkin-Elmer Instruments Co. Ltd, USA) by heating the samples in temperature range from room temperature to 700 °C under N_2 atmosphere with 10 °C min⁻¹ heating rate. Differential scanning calorimetry (DSC) was carried out with Pyris Diamond thermogravimetric/differential thermal analyzer (Perkin-Elmer Instruments Co. Ltd, USA) by heating the samples in temperature range from -20 to 300 °C under N_2 atmosphere with 10 °C min⁻¹ heating rate. Elemental analysis was performed on a Thermo Finnigan EA1112 Series Flash Elemental Analyzer (Thermo Finnigan, USA) and the content of bromide was determined by mercurimetric titration method. X-ray photoelectron spectra (XPS) experiments were carried out on a Thermo ESCALAB 250Xi analyzer (Thermo Fisher Scientific Inc., USA) using 300W Al K α radiation. The

Brunauer–Emmett–Teller (BET) specific surface area was calculated based on the Ar sorption isotherms measured at 87 K using a Quantachrome Instrument ASiQMVH002-5 (Quantachrome Instrument, USA), and pore size distribution profiles were calculated using non local density functional theory (NLDFT) model. Ionic conductivity of solid electrolytes was tested by Electrochemical Impedance Spectroscopy (EIS) by using electrochemical workstation (CHI660C, Chenhua, China) at different temperatures ranging from 303 to 423 K. Linear-sweep voltammetry (LSV) was implemented at room temperature with a sweep rate of 10 mV s⁻¹ from 1.5 to 6.0 V (versus Li⁺/Li) on an electrochemical workstation (CHI660C, Chenhua, China). Lithium ion transference number (t_{Li^+}) was tested by EIS analysis that was performed before and after potentiostatic direct current (DC) polarization, with the COF-based materials sandwiched between two lithium electrodes (CHI660C, Chenhua, China). The Li symmetric cell with Im-COF-TFSI@Li was assembled as Li|Im-COF-TFSI@Li|Li, and the polarization test was performed on a LAND battery test system (CT2001A, LANHE, China). The symmetric cells were tested by using a constant current density of 0.02 and 0.10 mA cm⁻², one charged/discharged process for 2 h. The thicknesses of COF pellets used for the electrochemical tests are 1.4 mm.

Synthesis of monomers



Scheme S1 Synthesis of TIBBr.

Synthesis of 1,3,5-tri(1*H*-imidazol-1-yl)benzene

The synthesis of 1,3,5-tri(1*H*-imidazol-1-yl)benzene has been reported.^{S1} A 10 mL Pyrex tube was charged with the mixture of 1,3,5-tribromobenzene (0.580 g, 1.84 mmol), imidazole (0.752 g, 11.05 mmol), K₂CO₃ (1.02 g, 7.37 mmol), and CuSO₄ (0.0147 g, 0.092 mmol), and was then vacuumed under room temperature for 30 min and subsequently sealed. The reaction was conducted at 180 °C for 24 h. After cooled to ambient temperature, the mixture was taken out from the glass tube and immersed into water (100 mL), followed with sonicating for 4 h. The residue was dissolved with ethanol and then filtrated to get a clear solution. After re-crystallization with ethanol and water, a white solid was obtained with yield 74%. ¹H NMR result is in good agreement with the literature. ¹H NMR (400 MHz, DMSO-*d*₆) δ = 8.55 (s, 3H) 8.04 (s, 3H), 7.97 (s, 3H), 7.19 (s, 3H) ppm. ¹³C NMR (101 MHz, DMSO-*d*₆) δ = 139.55, 136.54, 130.58, 118.78, 109.77 ppm.

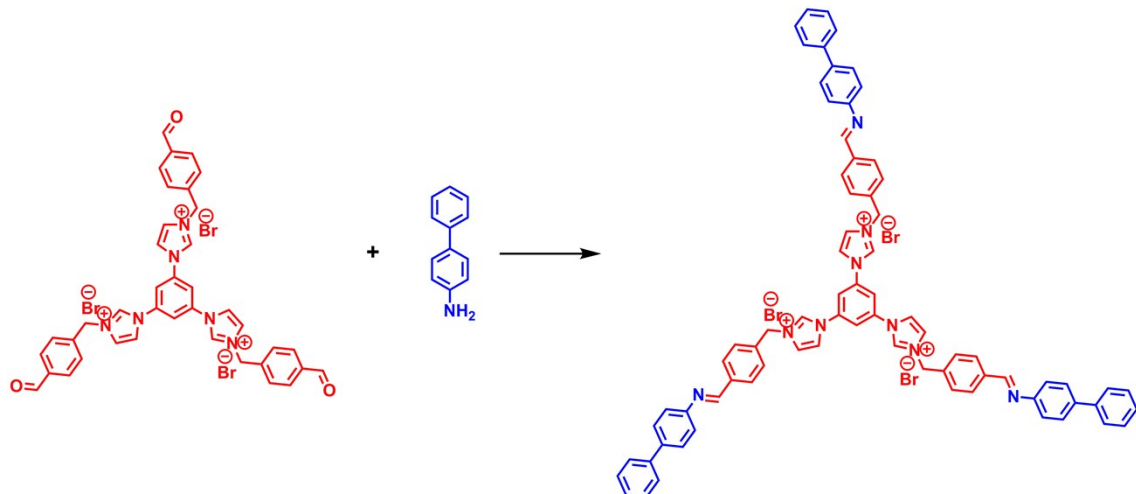
Synthesis of 4-(bromomethyl)benzaldehyde

The synthesis of the compound is based on a previous report.^{S2} A 500 mL flask was charged with 4-(bromomethyl)benzonitrile (5.0 g, 25.51 mmol), and vacuumed at ambient temperature for 2 h. Toluene (140 mL) was used to dissolve 4-(bromomethyl)benzonitrile, the obtained solution was then cooled to 0 °C and stirred under nitrogen atmosphere for 8 h. DIBAl-H (36.0 mL, 36.0 mmol, 1 M in hexanes) was added dropwise to the solution carefully, instantly, the solution turn yellow and clear. After stirred for 2 h, the solution was added with 66 mL CHCl₃ and then added with 200 mL 10 wt% HCl solution. The organic phase was separated from the mixture after stirring one more hour and washed with water for twice. The solution was dried with Na₂SO₄ and rotated under vacuum to give rise to pale yellow clear oil. After cooled down to ambient temperature, white solid could be immediately seen after addition of ice-cold hexane. The whole mixture was placed in refrigerator (4 °C) overnight and then filtrated to get the white crystals with yield of 84%. NMR results are in good agreement with literature. ¹H (400 MHz, CDCl₃) δ = 10.02 (s, 1H), 7.88 (d, *J* = 7.5 Hz, 2H), 7.57 (d, *J* = 7.5 Hz, 2H), 7.68 (d, *J* = 7.5 Hz, 1H), 7.54 (t, *J* = 7.5 Hz, 1H), 4.52 (s, 2H) ppm. ¹³C NMR (101 MHz, CDCl₃) δ = 191.50, 144.25, 136.14, 130.17, 129.68, 31.97 ppm.

Synthesis of 1,3,5-tris[3-(4-formylbenzyl)-1*H*-imidazol-1-yl]benzene bromide (TIBBr)

To a 50 mL glass flask charged with 1,3,5-tri(1*H*-imidazol-1-yl)benzene (276 mg, 1.0 mmol) and 4-(bromomethyl)benzaldehyde (895 mg, 4.5 mmol), added DMF (5 mL). The obtained solution was stirred for 30 min. After raising the temperature to 80 °C, a white solid precipitated out within few minutes from the solution, which was kept stirring for 24 h under the nitrogen atmosphere. After cooled down to the ambient temperature, the mixture was filtrated and washed with ethanol and followed with drying under vacuum. The product was collected with yield of 85%. ¹H NMR (400 MHz, DMSO-*d*₆) δ = 10.68 (s, 3H), 10.07 (d, *J* = 11.3 Hz, 3H), 8.80 (s, 3H), 8.74 (t, *J* = 1.7 Hz, 3H), 8.26 (m, 3H), 8.02 (d, *J* = 8.2 Hz, 6H), 7.82 (d, *J* = 8.1 Hz, 6H), 5.76 (s, 6H) ppm. ¹³C NMR (101 MHz, DMSO-*d*₆) δ = 193.32, 140.84, 137.21, 136.94, 130.53, 129.74, 124.33, 122.25, 116.67, 52.81 ppm. ESI-MS: calculated for [M–3Br]³⁺ = 211.1 (m/z), found 211.3.

Model reaction



Scheme S2 Synthesis of model compound.

To a round-bottomed flask charged with TIBBr (100 mg, 0.114 mmol) and 4-AB (67.6 mg, 0.4 mmol), 1,4-dioxane (16 mL), anhydrous methanol (4 mL), and acetic acid (0.15 mL) were added at room temperature. The reaction was refluxed for 24 h, and light yellow solids were obtained. The solids were recrystallized by methanol and washed by acetone, dried at 100 °C under vacuum for 12 h to yield final product as a light yellow powder. The product was collected with yield of 94%. ¹H NMR (400 MHz, DMSO-*d*₆) δ = 10.51 (s, 3H), 8.78 (s, 3H), 8.74 (d, *J* = 1.8 Hz, 3H), 8.64 (s, 3H), 8.24 (s, 3H), 8.06–8.08 (d, *J* = 7.9 Hz, 6H), 7.72 (d, *J* = 8.5 Hz, 6H), 7.49 (d, *J* = 7.3 Hz, 6H), 7.39–7.37 (d, *J* = 8.3 Hz, 6H), 7.35 (s, 6H), 7.22 (t, *J* = 7.3 Hz, 3H), 6.65 (s, 6H), 5.72 (s, 6H) ppm. ¹³C NMR (101 MHz, DMSO-*d*₆) δ = 162.21, 150.79, 140.88, 140.02, 138.73, 137.22, 130.56, 129.51, 127.78, 127.13, 125.85, 124.35, 122.17, 116.82, 52.75 ppm.

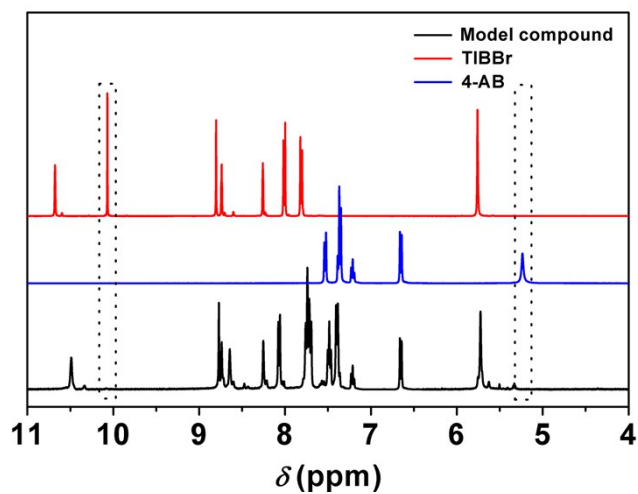


Fig. S1 ¹H NMR spectra of TIBBr, 4-AB, and model compound.

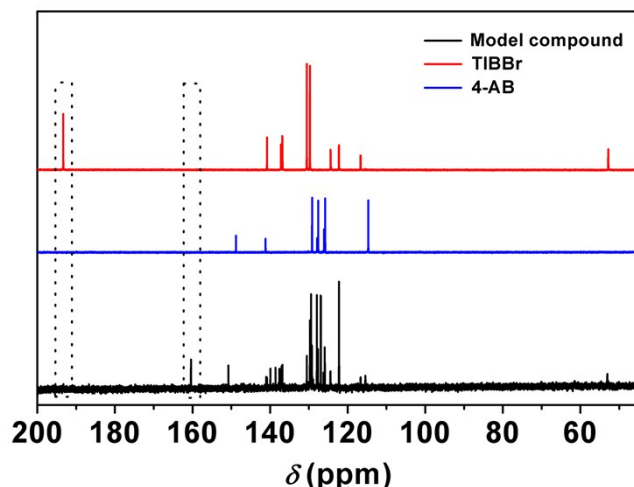


Fig. S2 ¹³C NMR spectra of TIBBr, 4-AB, and model compound.

Table S1 Element analysis results of Im-COF-Br and Im-COF-TFSI.

COFs	Calcd.				Found			
	C (%)	H (%)	N (%)	Br (%)	C (%)	H (%)	N (%)	Br (%)
Im-COF-Br	62.31	4.40	11.47	21.85	60.40	4.49	11.03	20.03
Im-COF-TFSI	44.53	2.85	9.89	—	44.88	2.99	9.84	—

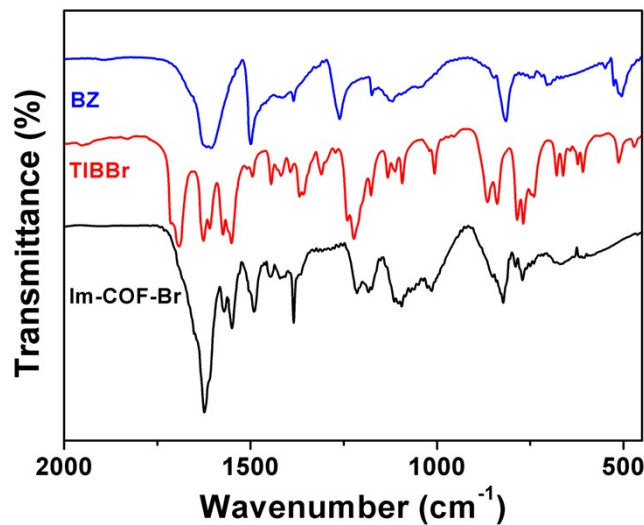


Fig. S3 FT-IR spectra of building block monomers and Im-COF-Br.

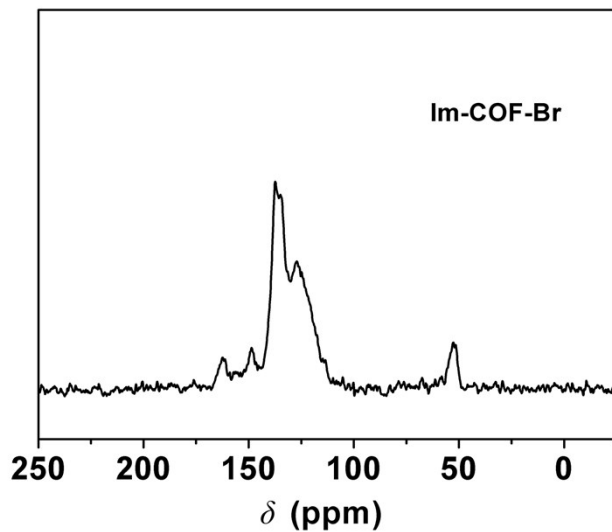


Fig. S4 Solid-state ¹³C NMR spectra of Im-COF-Br.

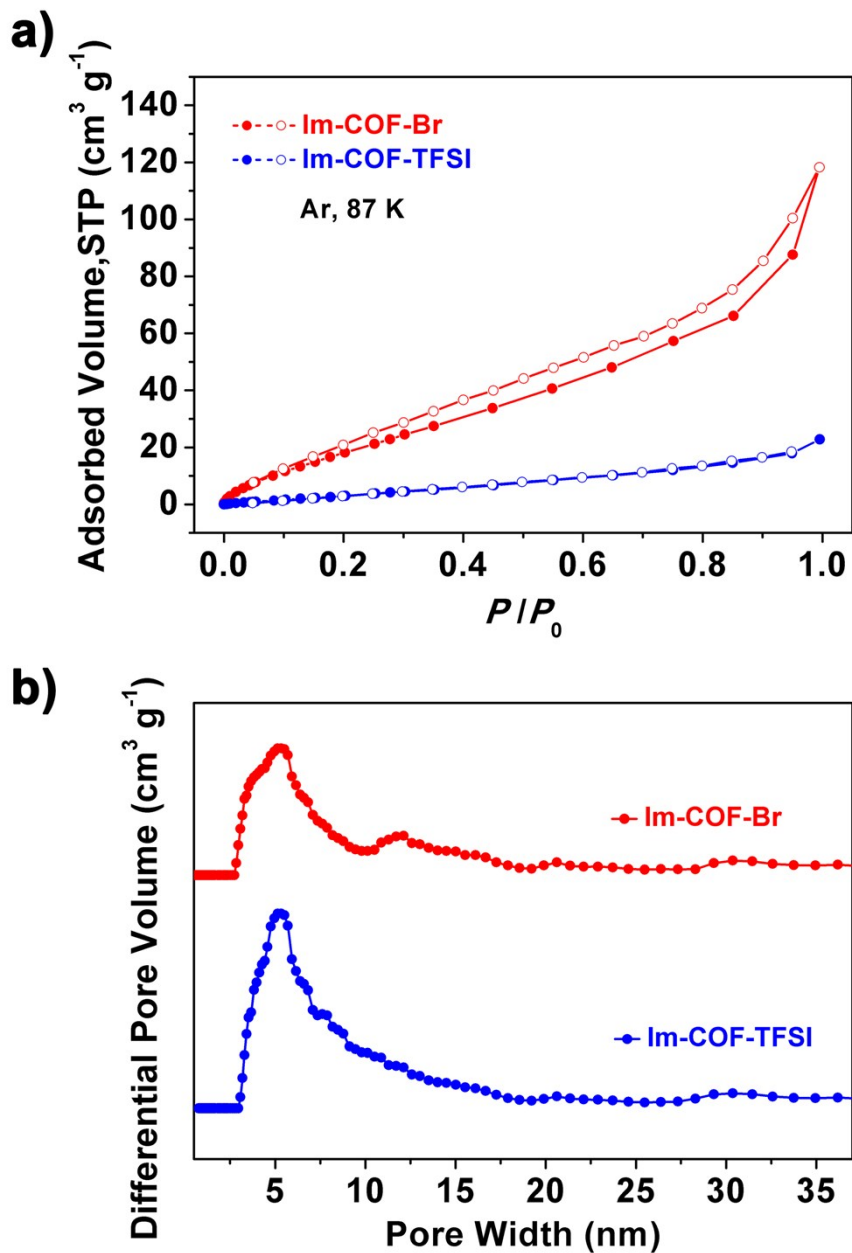


Fig. S5 (a) Argon-sorption isotherm curve of Im-COF-Br and Im-COF-TFSI measured at 87 K. (b) Pore size distribution profiles of Im-COF-Br and Im-COF-TFSI.

Structural modeling and powder X-ray diffraction analysis

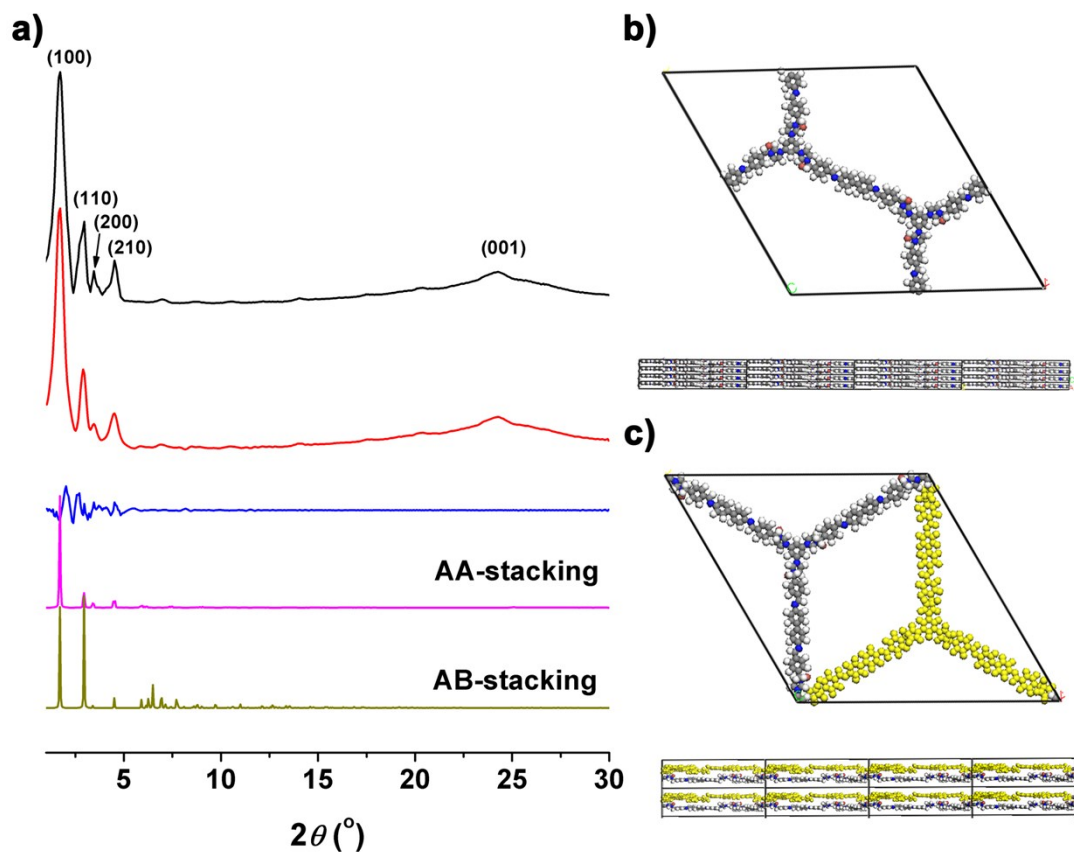


Fig. S6 (a) Experimental PXRD patterns of Im-COF-Br (black) compared with Pawley refined data (red), their difference (blue), simulated patterns using the eclipsed AA (magenta) and the staggered AB stacking mode (yellow). Top and side view of (b) AA and (c) AB stacking mode unit cell (C, grey; H, white; N, blue; Br, red).

Table S2 Refined crystal data for Im-COF-Br.

Crystal system	Triclinic
Space group	$P\bar{1}$
Unit cell dimensions	$a = 59.3332 \text{ \AA}$ $b = 60.0154 \text{ \AA}$ $c = 3.5577 \text{ \AA}$ $\alpha = 91.17^\circ$ $\beta = 89.80^\circ$ $\gamma = 118.94^\circ$
Pseudo-Voigt of peak profile function	$U = 0.16125$ $V = 0.53559$ $W = 0.14374$
Rietveld asymmetry correction	$P = 0.00704$
Pawley refinement	$R_{WP} = 9.78\%$ $R_p = 4.67\%$

Table S3 Atomistic coordinates for the refined unit cell parameters for Im-COF-Br via Pawley refinement.

Atom	x/a	y/b	z/c	Atom	x/a	y/b	z/c
C1	0.34850	0.68416	0.69252	C2	0.32157	0.67238	0.66814
N3	0.35828	0.62696	0.71316	C4	0.34675	0.60143	0.67685
N5	0.36417	0.59331	0.70273	C6	0.38726	0.61418	0.76232
C7	0.38361	0.63526	0.76667	C8	0.42414	0.76991	0.76058
C9	0.37925	0.56037	0.66376	C10	0.37312	0.53486	0.68440
C11	0.39234	0.52781	0.66264	C12	0.41825	0.54610	0.61824
C13	0.42524	0.57183	0.59227	C14	0.40657	0.57956	0.61158
C15	0.43844	0.53871	0.59998	C16	0.44409	0.48096	0.59517
C17	0.46206	0.47231	0.58642	C18	0.48985	0.49096	0.58042
C19	0.49711	0.51688	0.58230	C20	0.47851	0.52478	0.59022
C21	0.45210	0.50703	0.59708	N22	0.43296	0.51503	0.60980
C23	0.34868	0.68427	1.68380	C24	0.32176	0.67248	1.65939
N25	0.35848	0.62709	1.70466	C26	0.34699	0.60157	1.66818
N27	0.36443	0.59349	1.69422	C28	0.38751	0.61439	1.75417
C29	0.38382	0.63544	1.75847	C30	0.42432	0.77001	1.75171
C31	0.37951	0.56045	1.65371	C32	0.37315	0.53483	1.67594
C33	0.39225	0.52761	1.65447	C34	0.41807	0.54604	1.60935
C35	0.42455	0.57164	1.58365	C36	0.40538	0.57878	1.60410
C37	0.43851	0.53902	1.59077	C38	0.44507	0.48176	1.58642
C39	0.46349	0.47362	1.57827	C40	0.48987	0.49135	1.57223
C41	0.49742	0.51742	1.57346	C42	0.47900	0.52557	1.58104
C43	0.45267	0.50773	1.58793	N44	0.43331	0.51543	1.60068
C45	0.30665	0.64578	0.65853	C46	0.31899	0.63095	0.67251
N47	0.36363	0.71142	0.69782	C48	0.38935	0.72512	0.74069
N49	0.39708	0.75015	0.72903	C50	0.37575	0.75235	0.67305
C51	0.35480	0.72813	0.65519	C52	0.21912	0.63567	0.62754
C53	0.42972	0.79726	0.76802	C54	0.45542	0.81607	0.72991
C55	0.46218	0.84185	0.74050	C56	0.44319	0.84912	0.79080
C57	0.41753	0.83045	0.83293	C58	0.41086	0.80470	0.82342
C59	0.44969	0.87599	0.80053	C60	0.50654	0.93860	0.77472

C61	0.51410	0.96456	0.78184	C62	0.49566	0.97283	0.79658
C63	0.46946	0.95456	0.80390	C64	0.46189	0.92860	0.79750
C65	0.48045	0.92047	0.78312	N66	0.47333	0.89402	0.77650
C67	0.30684	0.64588	1.64979	C68	0.31917	0.63105	1.66382
N69	0.36380	0.71152	1.68910	C70	0.38952	0.72522	1.73195
N71	0.39725	0.75025	1.72024	C72	0.37592	0.75244	1.66426
C73	0.35498	0.72823	1.64644	C74	0.21937	0.63591	1.61854
C75	0.42988	0.79735	1.75913	C76	0.45558	0.81617	1.72095
C77	0.46233	0.84194	1.73152	C78	0.44333	0.84920	1.78185
C79	0.41768	0.83053	1.82403	C80	0.41102	0.80479	1.81455
C81	0.44982	0.87607	1.79160	C82	0.50662	0.93870	1.76586
C83	0.51416	0.96465	1.77300	C84	0.49570	0.97291	1.78774
C85	0.46952	0.95461	1.79504	C86	0.46196	0.92866	1.78862
C87	0.48054	0.92056	1.77423	N88	0.47345	0.89411	1.76758
C89	0.34588	0.64236	0.69834	C90	0.36047	0.66899	0.70872
N91	0.27908	0.63385	0.63677	C92	0.26473	0.64565	0.64765
N93	0.23955	0.62856	0.62544	C94	0.23794	0.60537	0.59709
C95	0.26265	0.60865	0.60542	C96	0.35735	0.56636	0.68339
C97	0.19158	0.61440	0.63205	C98	0.17221	0.62131	0.61643
C99	0.14625	0.60277	0.62155	C100	0.13933	0.57697	0.64294
C101	0.15855	0.56993	0.66028	C102	0.18448	0.58852	0.65572
C103	0.11228	0.55709	0.64602	C104	0.04842	0.55160	0.63677
C105	0.02227	0.53362	0.63440	C106	0.01433	0.50745	0.63253
C107	0.03315	0.49967	0.63365	C108	0.05931	0.51763	0.63637
C109	0.06709	0.54376	0.63775	N110	0.09373	0.56265	0.63779
C111	0.34606	0.64248	1.68969	C112	0.36065	0.66910	1.70005
N113	0.27927	0.63397	1.62804	C114	0.26495	0.64581	1.63883
N115	0.23977	0.62875	1.61656	C116	0.23812	0.60554	1.58826
C117	0.26281	0.60879	1.59669	C118	0.35764	0.56653	1.67478
C119	0.19183	0.61467	1.62314	C120	0.17247	0.62160	1.60748
C121	0.14650	0.60309	1.61265	C122	0.13958	0.57728	1.63414
C123	0.15878	0.57022	1.65153	C124	0.18470	0.58879	1.64691
C125	0.11254	0.55740	1.63724	C126	0.04854	0.55154	1.62783
C127	0.02243	0.53341	1.62539	C128	0.01469	0.50729	1.62355

C129	0.03367	0.49971	1.62482	C130	0.05976	0.51781	1.62760
C131	0.06735	0.54389	1.62892	N132	0.09395	0.56290	1.62897
C133	0.65083	0.28945	0.53825	C134	0.67775	0.30126	0.51849
N135	0.64096	0.34660	0.59967	C136	0.65244	0.37212	0.57955
N137	0.63500	0.38020	0.61347	C138	0.61192	0.35930	0.66186
C139	0.61562	0.33825	0.65098	C140	0.57522	0.20369	0.55547
C141	0.61997	0.41328	0.59797	C142	0.62640	0.43892	0.63758
C143	0.60736	0.44622	0.62313	C144	0.58152	0.42785	0.56761
C145	0.57497	0.40223	0.52453	C146	0.59409	0.39501	0.53806
C147	0.56115	0.43499	0.55614	C148	0.55523	0.49259	0.59278
C149	0.53723	0.50119	0.59221	C150	0.50945	0.48250	0.57630
C151	0.50223	0.45660	0.56073	C152	0.52087	0.44874	0.56091
C153	0.54727	0.46654	0.57722	N154	0.56648	0.45862	0.58232
C155	0.65068	0.28961	1.52992	C156	0.67766	0.30144	1.51015
N157	0.64021	0.34640	1.59161	C158	0.65181	0.37191	1.57134
N159	0.63447	0.38010	1.60578	C160	0.61135	0.35927	1.65479
C161	0.61490	0.33813	1.64366	C162	0.57521	0.20376	1.54639
C163	0.61956	0.41313	1.58986	C164	0.62570	0.43863	1.62815
C165	0.60648	0.44569	1.61277	C166	0.58059	0.42739	1.55730
C167	0.57360	0.40168	1.51331	C168	0.59226	0.39395	1.52564
C169	0.56037	0.43473	1.54637	C170	0.55415	0.49216	1.58383
C171	0.53576	0.50036	1.58357	C172	0.50937	0.48267	1.56803
C173	0.50178	0.45659	1.55169	C174	0.52014	0.44839	1.55136
C175	0.54649	0.46618	1.56782	N176	0.56578	0.45837	1.57276
C177	0.69265	0.32787	0.52517	C178	0.68029	0.34268	0.55095
N179	0.63573	0.26220	0.52668	C180	0.61000	0.24848	0.56275
N181	0.60229	0.22346	0.53483	C182	0.62363	0.22127	0.47530
C183	0.64457	0.24550	0.47183	C184	0.78019	0.33800	0.49109
C185	0.56965	0.17634	0.54471	C186	0.54395	0.15753	0.49713
C187	0.53719	0.13176	0.49070	C188	0.55618	0.12449	0.53322
C189	0.58185	0.14316	0.58467	C190	0.58852	0.16890	0.59215
C191	0.54968	0.09762	0.52515	C192	0.49283	0.03502	0.46324
C193	0.48526	0.00905	0.45328	C194	0.50370	0.00078	0.45996
C195	0.52990	0.01905	0.47669	C196	0.53748	0.04501	0.48736

C197	0.51892	0.05313	0.48094	N198	0.52604	0.07958	0.49176
C199	0.69288	0.32802	1.51614	C200	0.68095	0.34314	1.54124
N201	0.63565	0.26233	1.51838	C202	0.60993	0.24856	1.55415
N203	0.60226	0.22355	1.52621	C204	0.62364	0.22142	1.46695
C205	0.64455	0.24567	1.46366	C206	0.78028	0.33764	1.48257
C207	0.56964	0.17642	1.53566	C208	0.54393	0.15760	1.48835
C209	0.53717	0.13183	1.48198	C210	0.55616	0.12456	1.52430
C211	0.58183	0.14323	1.57546	C212	0.58851	0.16898	1.58284
C213	0.54966	0.09769	1.51625	C214	0.49282	0.03506	1.45445
C215	0.48527	0.00910	1.44448	C216	0.50373	0.00084	1.45114
C217	0.52992	0.01913	1.46787	C218	0.53748	0.04508	1.47854
C219	0.51891	0.05320	1.47214	N220	0.52602	0.07965	1.48296
C221	0.65340	0.33123	0.57250	C222	0.63884	0.30460	0.56646
N223	0.72022	0.33981	0.50808	C224	0.73459	0.32802	0.50971
N225	0.75976	0.34511	0.49589	C226	0.76136	0.36830	0.48240
C227	0.73665	0.36501	0.49131	C228	0.64181	0.40716	0.61244
C229	0.80773	0.35927	0.50705	C230	0.82709	0.35235	0.48432
C231	0.85306	0.37088	0.49920	C232	0.85998	0.39669	0.53769
C233	0.84077	0.40374	0.56224	C234	0.81484	0.38515	0.54788
C235	0.88704	0.41656	0.55134	C236	0.95089	0.42203	0.53848
C237	0.97705	0.44001	0.54533	C238	0.98499	0.46617	0.56043
C239	0.96617	0.47396	0.56914	C240	0.94002	0.45600	0.56264
C241	0.93223	0.42987	0.54703	N242	0.90559	0.41099	0.53717
C243	0.65266	0.33108	1.56435	C244	0.63842	0.30452	1.55815
N245	0.72043	0.33970	1.49850	C246	0.73467	0.32778	1.50097
N247	0.75988	0.34479	1.48664	C248	0.76160	0.36802	1.47197
C249	0.73697	0.36487	1.48074	C250	0.64140	0.40708	1.60453
C251	0.80782	0.35893	1.49822	C252	0.82721	0.35206	1.47513
C253	0.85316	0.37063	1.48986	C254	0.86005	0.39643	1.52853
C255	0.84081	0.40343	1.55347	C256	0.81490	0.38481	1.53930
C257	0.88709	0.41632	1.54230	C258	0.95196	0.42139	1.52933
C259	0.97790	0.43973	1.53623	C260	0.98541	0.46580	1.55130
C261	0.96645	0.47345	1.56001	C262	0.94025	0.45567	1.55370
C263	0.93225	0.42957	1.53825	N264	0.90561	0.41072	1.52808

H265	0.31155	0.68445	0.65587	H266	0.32503	0.58997	0.63116
H267	0.40526	0.61214	0.79840	H268	0.40075	0.65512	0.81057
H269	0.43252	0.76654	1.02772	H270	0.43415	0.76649	0.50946
H271	0.35222	0.51951	0.71941	H272	0.38706	0.50690	0.68098
H273	0.44632	0.58665	0.55507	H274	0.41239	0.60057	0.58720
H275	0.45950	0.55393	0.57662	H276	0.42262	0.46672	0.60084
H277	0.45530	0.45100	0.58393	H278	0.51838	0.53175	0.57734
H279	0.48464	0.54595	0.59120	H280	0.31173	0.68456	1.64708
H281	0.32527	0.59008	1.62226	H282	0.40552	0.61238	1.79051
H283	0.40093	0.65531	1.80258	H284	0.43270	0.76664	2.01884
H285	0.43433	0.76659	1.50057	H286	0.35221	0.51961	1.71191
H287	0.38684	0.50667	1.67368	H288	0.44551	0.58676	1.54592
H289	0.41069	0.59967	1.58044	H290	0.45948	0.55444	1.56711
H291	0.42371	0.46719	1.59189	H292	0.45717	0.45240	1.57647
H293	0.51874	0.53214	1.56825	H294	0.48534	0.54679	1.58165
H295	0.30714	0.60928	0.66289	H296	0.40124	0.71505	0.77978
H297	0.37740	0.77200	0.64949	H298	0.33462	0.72547	0.61100
H299	0.22225	0.64862	0.88340	H300	0.22240	0.64739	0.36475
H301	0.47108	0.81043	0.68977	H302	0.48318	0.85701	0.70818
H303	0.40197	0.83621	0.87518	H304	0.38993	0.78951	0.86085
H305	0.43380	0.88140	0.82976	H306	0.52168	0.93210	0.76200
H307	0.53542	0.97925	0.77567	H308	0.45417	0.96086	0.81516
H309	0.44056	0.91392	0.80395	H310	0.30732	0.60939	1.65421
H311	0.40141	0.71515	1.77105	H312	0.37757	0.77209	1.64067
H313	0.33480	0.72557	1.60226	H314	0.22253	0.64887	1.87432
H315	0.22267	0.64762	1.35566	H316	0.47125	0.81054	1.68078
H317	0.48332	0.85711	1.69916	H318	0.40211	0.83628	1.86630
H319	0.39009	0.78959	1.85204	H320	0.43391	0.88146	1.82083
H321	0.52179	0.93222	1.75314	H322	0.53548	0.97936	1.76685
H323	0.45420	0.96089	1.80631	H324	0.44065	0.91396	1.79506
H325	0.38236	0.67857	0.73059	H326	0.27446	0.66731	0.67268
H327	0.21830	0.58756	0.57207	H328	0.26582	0.59139	0.58667
H329	0.34526	0.55668	0.94012	H330	0.34462	0.55815	0.42264
H331	0.17754	0.64223	0.59933	H332	0.13065	0.60864	0.60831

H333	0.15309	0.54897	0.67821	H334	0.20013	0.58273	0.67131
H335	0.10717	0.53619	0.65584	H336	0.05463	0.57279	0.63790
H337	0.00714	0.54014	0.63398	H338	0.02715	0.47852	0.63235
H339	0.07443	0.51110	0.63746	H340	0.38254	0.67869	1.72195
H341	0.27471	0.66746	1.66384	H342	0.21847	0.58775	1.56320
H343	0.26596	0.59150	1.57799	H344	0.34561	0.55686	1.93190
H345	0.34485	0.55834	1.41466	H346	0.17783	0.64254	1.59031
H347	0.13092	0.60897	1.59937	H348	0.15330	0.54926	1.66953
H349	0.20034	0.58298	1.66254	H350	0.10744	0.53650	1.64712
H351	0.05459	0.57270	1.62894	H352	0.00717	0.53977	1.62488
H353	0.02783	0.47860	1.62359	H354	0.07500	0.51143	1.62880
H355	0.68780	0.28921	0.49665	H356	0.67415	0.38361	0.53887
H357	0.59391	0.36131	0.70196	H358	0.59851	0.31838	0.68345
H359	0.56682	0.20705	0.82572	H360	0.56523	0.20711	0.30767
H361	0.64735	0.45410	0.68215	H362	0.61283	0.46717	0.65657
H363	0.55400	0.38716	0.47822	H364	0.58872	0.37411	0.50026
H365	0.54016	0.41964	0.52367	H366	0.57669	0.50686	0.60602
H367	0.54395	0.52249	0.60395	H368	0.48097	0.44169	0.54775
H369	0.51479	0.42758	0.54768	H370	0.68770	0.28939	1.48861
H371	0.67353	0.38330	1.53013	H372	0.59340	0.36139	1.69552
H373	0.59773	0.31831	1.67654	H374	0.56677	0.20711	1.81644
H375	0.56523	0.20718	1.29838	H376	0.64659	0.45397	1.67254
H377	0.61175	0.46659	1.64552	H378	0.55253	0.38688	1.46702
H379	0.58646	0.37295	1.48634	H380	0.53934	0.41949	1.51403
H381	0.57552	0.50670	1.59714	H382	0.54213	0.52159	1.59606
H383	0.48045	0.44190	1.53853	H384	0.51377	0.42716	1.53768
H385	0.69212	0.36434	0.55460	H386	0.59810	0.25855	0.60985
H387	0.62199	0.20163	0.43858	H388	0.66475	0.24816	0.42746
H389	0.77705	0.32506	0.73856	H390	0.77692	0.32627	0.22076
H391	0.52828	0.16317	0.46315	H392	0.51619	0.11660	0.45080
H393	0.59741	0.13740	0.62067	H394	0.60945	0.18410	0.63713
H395	0.56557	0.09221	0.54848	H396	0.47768	0.04151	0.45693
H397	0.46394	-0.00564	0.43959	H398	0.54520	0.01275	0.48168
H399	0.55880	0.05969	0.50134	H400	0.69308	0.36477	1.54384

H401	0.59798	0.25857	1.60107	H402	0.62205	0.20179	1.43028
H403	0.66475	0.24839	1.41950	H404	0.77714	0.32475	1.73063
H405	0.77702	0.32587	1.21267	H406	0.52827	0.16324	1.45455
H407	0.51617	0.11667	1.44228	H408	0.59740	0.13747	1.61129
H409	0.60945	0.18417	1.62752	H410	0.56555	0.09227	1.53953
H411	0.47767	0.04155	1.44815	H412	0.46395	-0.00560	1.43079
H413	0.54523	0.01285	1.47284	H414	0.55880	0.05978	1.49251
H415	0.61695	0.29499	0.58460	H416	0.72486	0.30637	0.52170
H417	0.78100	0.38611	0.46678	H418	0.73347	0.38226	0.48413
H419	0.65382	0.41680	0.87512	H420	0.65463	0.41537	0.35681
H421	0.82175	0.33143	0.45332	H422	0.86865	0.36500	0.48001
H423	0.84624	0.42469	0.59408	H424	0.79919	0.39095	0.56940
H425	0.89216	0.43746	0.57493	H426	0.94468	0.40084	0.52584
H427	0.99218	0.43348	0.53867	H428	0.97218	0.49511	0.58163
H429	0.92489	0.46254	0.57001	H430	0.61652	0.29469	1.57615
H431	0.72483	0.30613	1.51392	H432	0.78128	0.38576	1.45567
H433	0.73389	0.38219	1.47270	H434	0.65340	0.41670	1.86742
H435	0.65422	0.41530	1.34887	H436	0.82191	0.33114	1.44397
H437	0.86879	0.36479	1.47040	H438	0.84624	0.42438	1.58546
H439	0.79922	0.39056	1.56119	H440	0.89218	0.43721	1.56600
H441	0.94621	0.40030	1.51689	H442	0.99337	0.43365	1.52965
H443	0.97234	0.49457	1.57250	H444	0.92527	0.46240	1.56114
Br445	0.42366	0.74200	0.79499	Br446	0.24941	0.66255	0.75817
Br447	0.33147	0.56908	0.52142	Br448	0.66814	0.40335	0.79313
Br449	0.75357	0.31194	0.37796	Br450	0.57935	0.23658	0.49572

Table S4 Elements tested by XPS spectra (Atom%).

	C 1s	O 1s	N 1s	Br 3d	S 2s&2p	F 1s
Im-COF-Br	77.06	4.24	14.47	4.23	—	—
Im-COF-TFSI	53.37	12.93	10.25	0.01	5.19	19.00

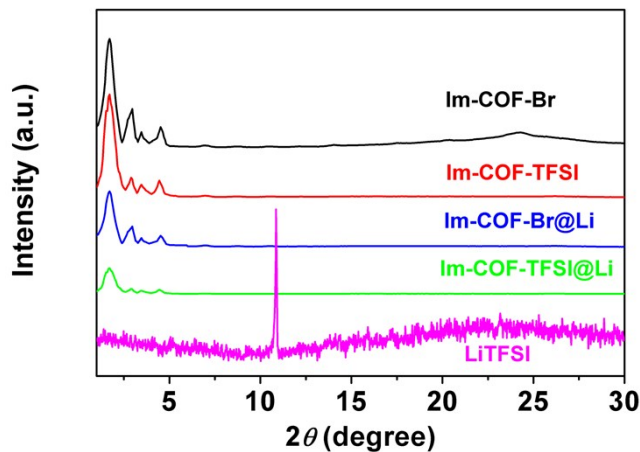


Fig. S7 PXRD patterns of LiTFSI, Im-COF-Br, Im-COF-TFSI, Im-COF-Br@Li and Im-COF-TFSI@Li.

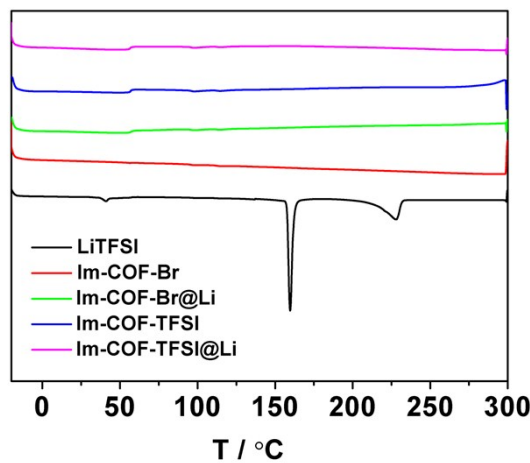


Fig. S8 DSC profiles of LiTFSI, Im-COF-Br, Im-COF-TFSI, Im-COF-Br@Li and Im-COF-TFSI@Li.

Preparation of Im-COF-TFSI@Li pellet

The electrolyte pellet was obtained by pressing the Im-COF-TFSI@Li powder (Im-COF-TFSI 100 mg, LiTFSI 100 mg) at 10 MPa for 10 min. A pellet was obtained and further dried under vacuum at 80 °C to remove any residual moisture before measurement. All the processes for preparing the pellet were performed in an Ar-filled dry box.



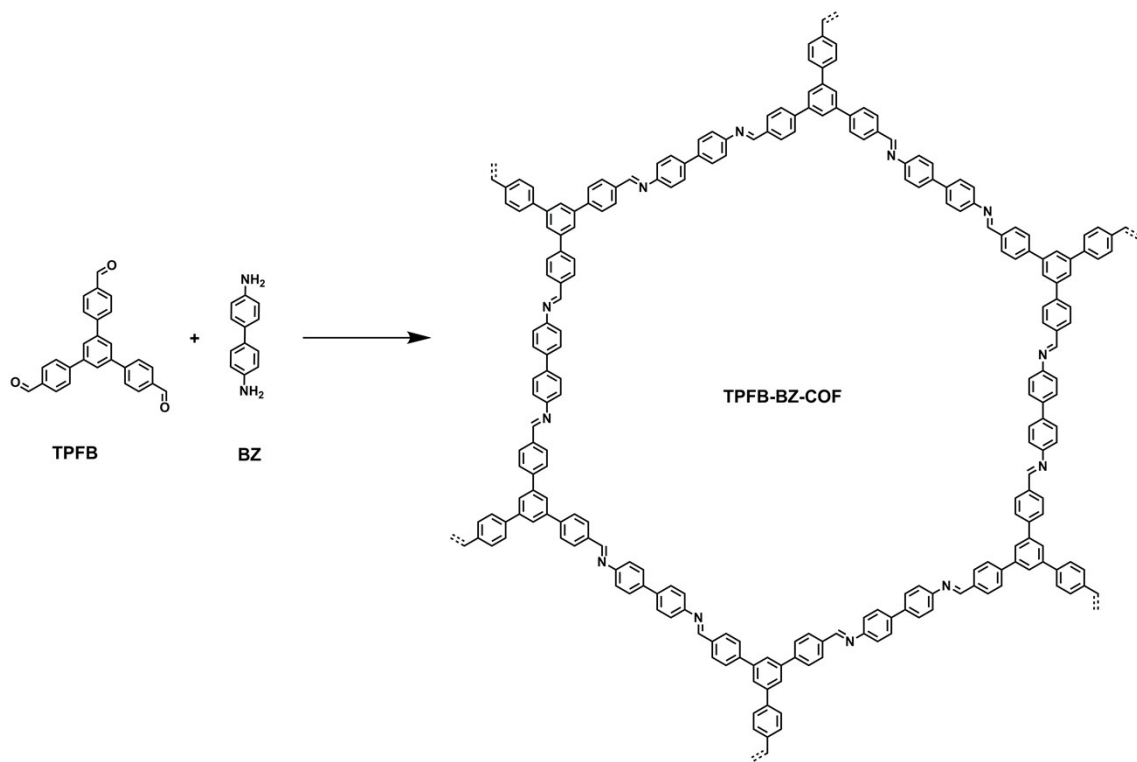
Fig. S9 A photo of Im-COF-TFSI@Li pellet.

Assembly and performance testing of Li/Im-COF-TFSI@Li/LiFePO₄ cell

The cathode were fabricated by mixing of LiFePO₄ (70 wt%), super P (20 wt%) and PVDF (10 wt%, binder) to form a viscous slurry that was then cast onto Al foil. Cells were prepared in an Ar-filled glove box by placing LiFePO₄ cathode, Im-COF-TFSI@Li electrolyte and Li metal in a CR2032 button cell. A LANHE CT2001A battery testing system was used for all the tests of the all-solid-state cells at the current density of 0.1 C under 353 K with the voltage range from 2.5 to 4.0 V.

Synthesis of TPFB-BZ-COF and TPFB-BZ-COF@Li

The building blocks TPFB (0.08 mmol) and BZ (0.12 mmol) were dissolved in a mixture solvent of 1,4-dioxane (1.0 mL), mesitylene (1 mL), and aqueous acetic acid (3.0 M, 0.2 mL), and then added into glass tube. The condensation reaction system was kept in 120 °C oven for 3 days undisturbedly. The precipitate was collected by centrifugation, washed with anhydrous THF and acetone, and dried under vacuum at 80 °C for 24 h. The final product was obtained as yellow solid powder with a yield of 91%. TPFB-BZ-COF@Li was prepared by mixing TPFB-BZ-COF and LiTFSI in ethanol solvent uniformly and then drying it at 80 °C under vacuum for 12 h.



Scheme S3 Synthesis of TPFB-BZ-COF.

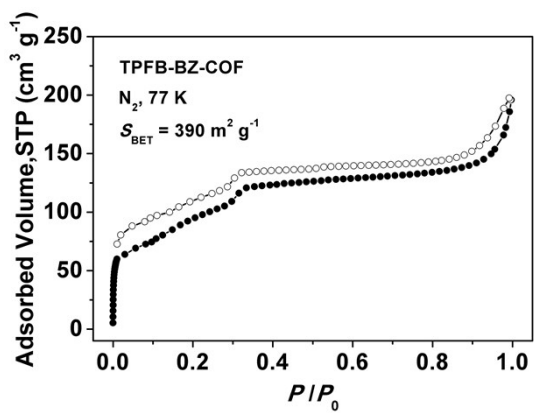


Fig. S10 Nitrogen sorption isotherm curve of TPFB-BZ-COF measured at 77 K.

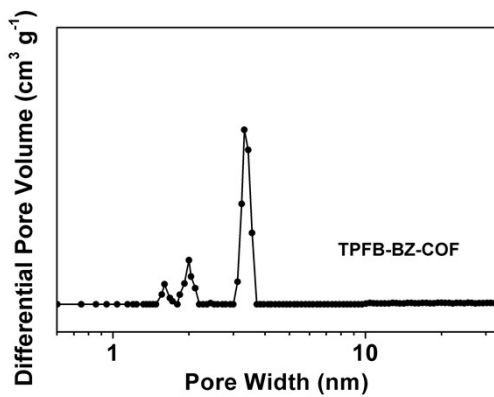


Fig. S11 Pore size distribution profile of TPFB-BZ-COF.

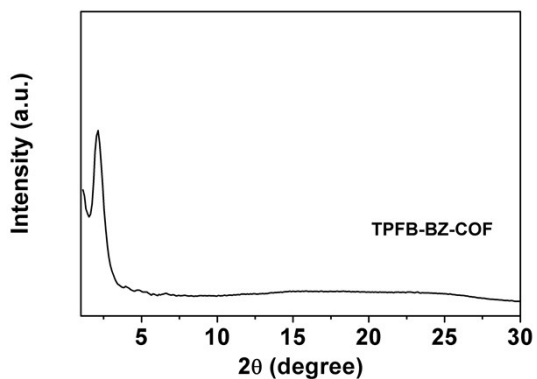


Fig. S12 PXRD pattern of TPFB-BZ-COF.

Preparation of TPFB-BZ-COF@Li and Im-COF-Br@Li pellet

The electrolyte pellet of TPFB-BZ-COF@Li and Im-COF-Br@Li were obtained by utilizing similar procedure with the preparation of Im-COF-TFSI@Li pellet.

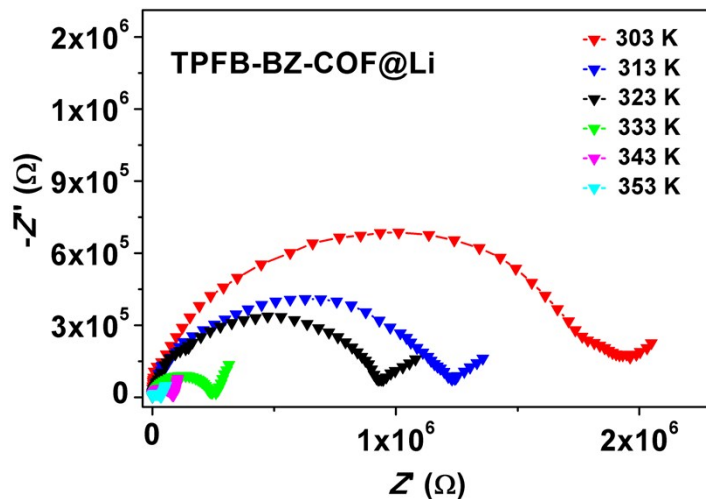


Fig. S13 Nyquist plots of TPFB-BZ-COF@Li measured at 303, 313, 323, 333, 343, and 353 K, respectively.

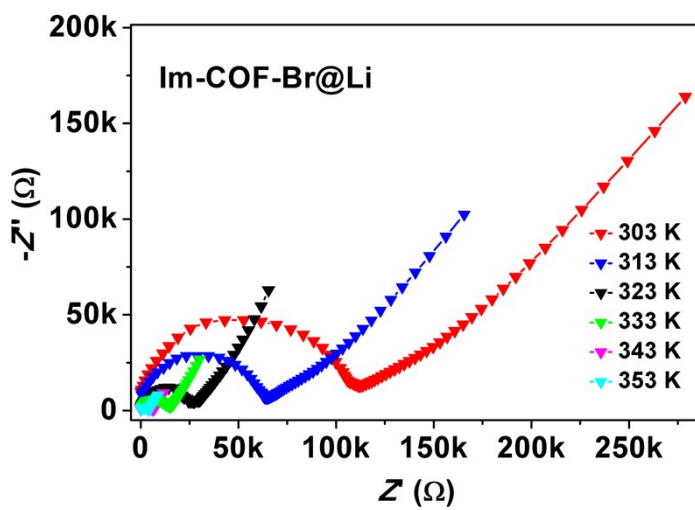


Fig. S14 Nyquist plots of Im-COF-Br@Li measured at 303, 313, 323, 333, 343, and 353 K, respectively.

Table S5 Summary of the typical performances of porous polymer based Li⁺ all-solid or solid-like electrolytes.

Materials	Conductivity (S cm ⁻¹)	Description	Year	Ref
LiO'Pr into MOF	3.1×10^{-4} (300 K)	MOF&liquid organic molecule (solid-like)	2011	S3
LiOtBu-grafted UiO-66	1.8×10^{-5} (RT)	MOF+surface modification (all-solid)	2013	S4
PEO+LiTFSI+Al-BTC (MOF)	10^{-6} (295 K)	MOF+polymer (all-solid)	2014	S5
Cu(II)-azolate MOF	4.8×10^{-4} (RT)	MOF+LiBF ₄ (all-solid)	2017	S6
LPC@UiO-67	10^{-3} (RT)	MOF+ LiClO ₄ (solid-like)	2018	S7
MOF-525	3.0×10^{-4} (RT)	Li-IL@MOF (solid-like)	2018	S8
UiO-67	1.0×10^{-4} (RT)	LLZO+MOF (solid-like)	2018	S9
MOF-MX _n	1.1×10^{-4} (298 K)	MOF+LiI (all-solid)	2019	S10
UiO-66	3.2×10^{-4} (298 K)	MOF+Li-IL (solid-like)	2019	S11
Al-Td-MOF-1	5.7×10^{-5} (RT)	Anionic aluminum MOF (all-solid)	2019	S12
Porous organic cage	1.0×10^{-3} (RT)	Porous organic cage+LiTFSI+DME (solid-like)	2018	S13
ICOF with spiroborate linkage	3.05×10^{-5} (RT)	ICOF linked by spiroborate (all-solid)	2016	S14
COF-5 with mechanically shaped	2.6×10^{-4} (RT)	Mechanically COFs (all-solid)	2016	S15
3D anionic CD-COF	2.7×10^{-3} (303 K)	CD-COF-Li \supset LiPF ₆ -EC-DMC (solid-like)	2017	S16
Guanidinium-based 2D ion-CONs	5.74×10^{-5} (300 K) 2.09×10^{-4} (343 K)	CON+LiTFSI (all-solid)	2018	S17
2D COF with oligo(ethylene oxide) chains	6.04×10^{-6} (313 K) 1.66×10^{-4} (353 K)	COF+ LiClO ₄ (all-solid)	2018	S18
COF-PEO-9-Li	7.94×10^{-6} (373 K) 1.33×10^{-3} (473 K)	COF+LiTFSI (all-solid)	2019	S19
PEG-Li ⁺ @EB-COF-ClO ₄	1.93×10^{-5} (303 K) 1.78×10^{-3} (393 K)	PEG+LiClO ₄ + EB-COF-ClO ₄ (all-solid)	2019	S20

PVDF/H-COF-1@10 film	2.5×10^{-4} (RT)	PVDF+ LiClO ₄ +COF-1 (all-solid)	2019	S21
Lithium sulfonated COF	2.7×10^{-5} (RT)	TpPa-SO ₃ Li (all-solid)	2019	S22
CF ₃ -Li-ImCOF	7.2×10^{-3} (RT)	Li ⁺ +anionic ICOF+20 wt % PC (solid-like)	2019	S23
Im-COF-TFSI	2.92×10^{-5} (303 K) 4.64×10^{-4} (353 K) 4.04×10^{-3} (423 K)	COF+LiTFSI (all-solid)	2019	This work
Im-COF-Br	8.34×10^{-7} (303 K) 3.63×10^{-5} (353 K)	COF+LiTFSI (all-solid)	2019	This work
TPFB-BZ-COF	7.56×10^{-9} (303 K) 4.26×10^{-7} (353 K)	COF+LiTFSI (all-solid)	2019	This work

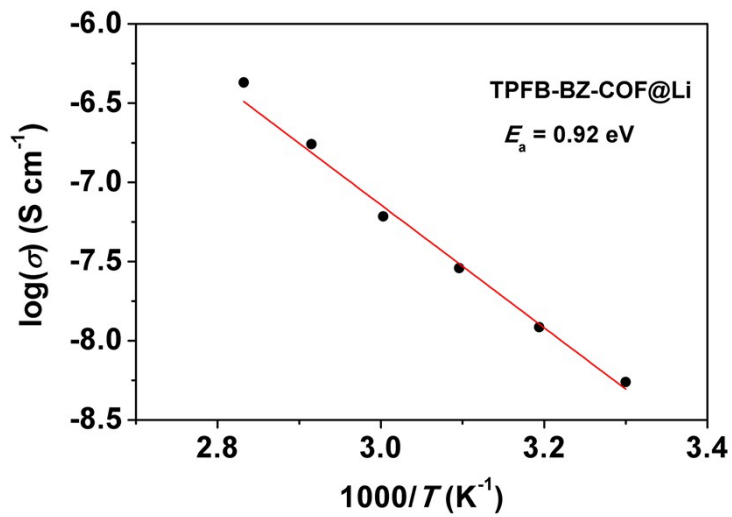


Fig. S15 Arrhenius plot of the TPFB-BZ-COF@Li ionic conductivity.

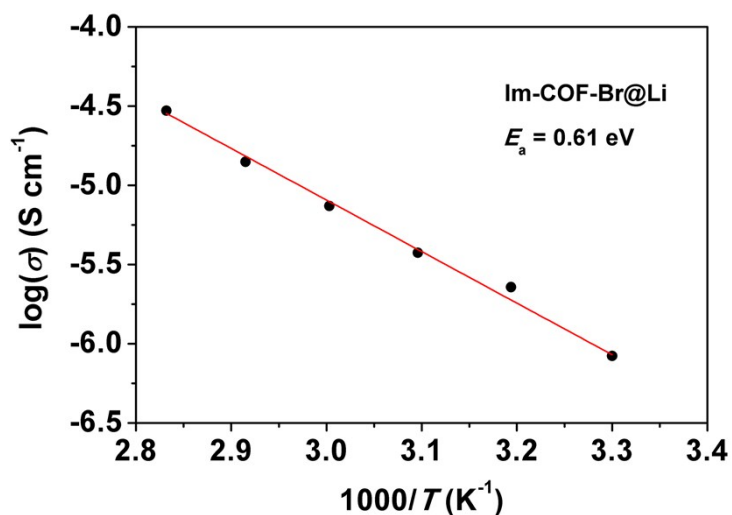


Fig. S16 Arrhenius plot of the Im-COF-Br@Li ionic conductivity.

Table S6 Summary of the activation energy (E_a) of COF-based Li⁺ electrolytes.

Materials	E_a (ev)	Year	Ref
ICOF with spiroborate linkage (all-solid)	0.24	2016	S14
COF-5 with mechanically shaped (all-solid)	0.04	2016	S15
3D anionic CD-COF (solid-like)	0.26	2017	S16
Guanidinium-based 2D ion-CONs (all-solid)	0.34	2018	S17
2D COF with oligo(ethylene oxide) chains (all-solid)	0.87	2018	S18
PEG-Li ⁺ @EB-COF-ClO ₄ (all-solid)	0.21	2019	S20
TpPa-SO ₃ Li (all-solid)	0.18	2019	S22
CF ₃ -Li-ImCOF (solid-like)	0.10	2019	S23
TPFB-BZ-COF@Li (all-solid)	0.92	2019	This work
Im-COF-Br@Li (all-solid)	0.61	2019	This work
Im-COF-TFSI@Li (all-solid)	0.32	2019	This work

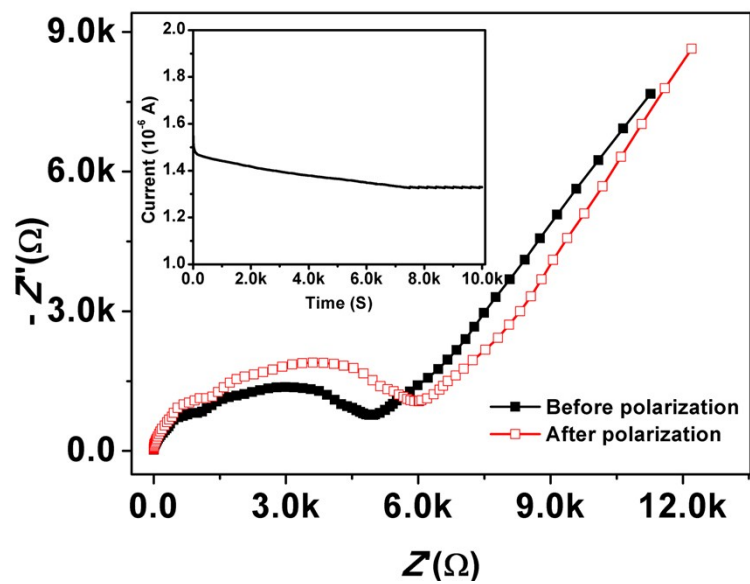


Fig. S17 EIS results of symmetric cell before and after polarization under 303 K. Inset: Time-dependent current of Im-COF-TFSI@Li before and after DC polarization (with a DC voltage of 50 mV).

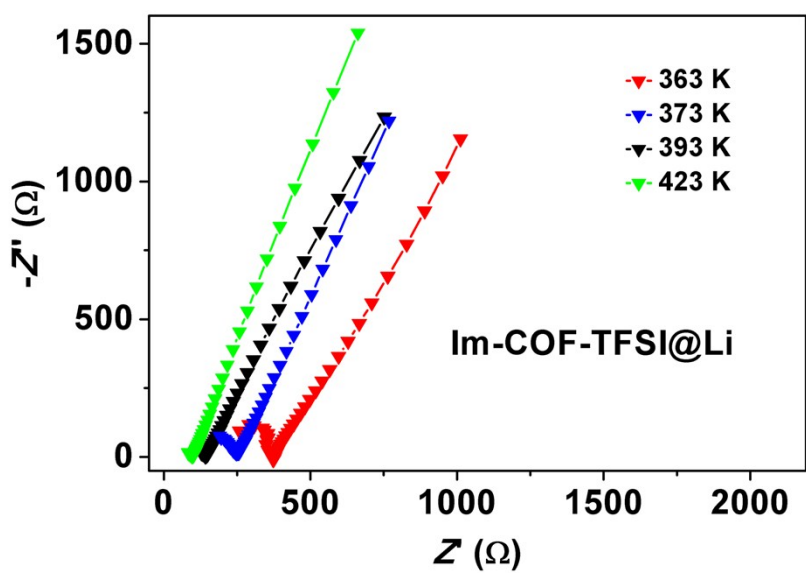


Fig. S18 Nyquist plots of Im-COF-TFSI@Li measured at 363, 373, 393, and 423 K, respectively.

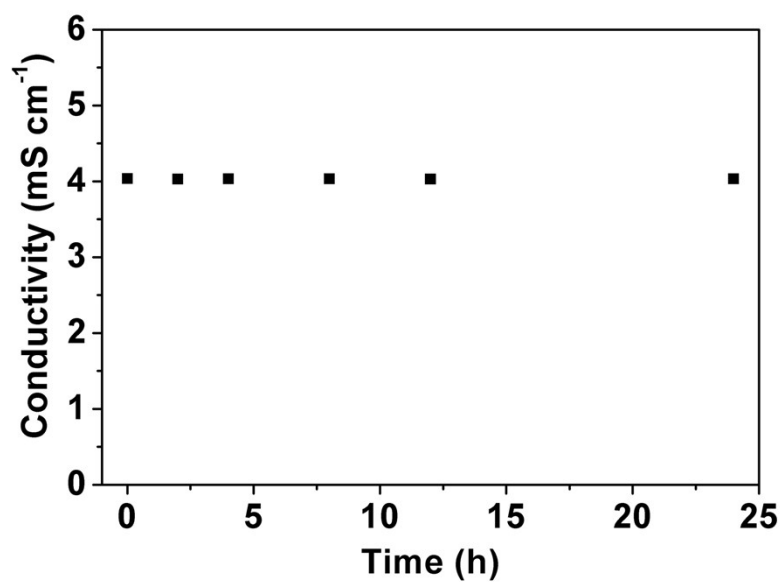


Fig. S19 Time course Li^+ conductivity of Im-COF-TFSI@Li measured at 423 K.

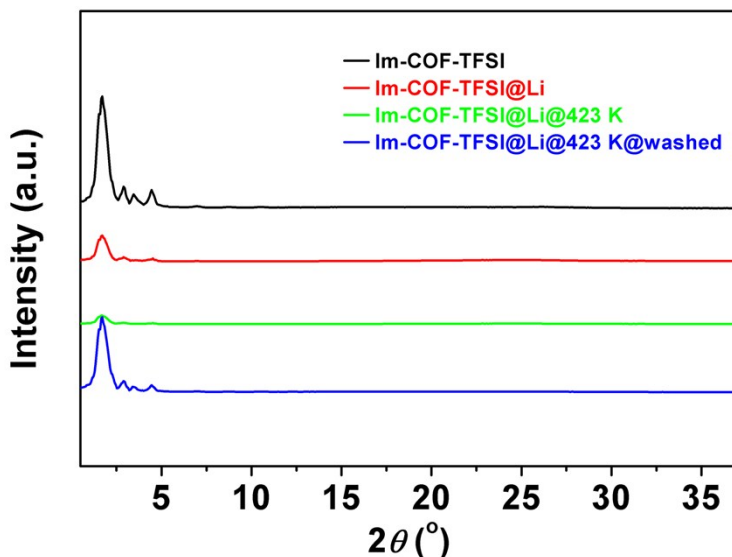


Fig. S20 PXRD patterns of Im-COF-TFSI, Im-COF-TFSI@Li, Im-COF-TFSI@Li@423K, and Im-COF-TFSI@Li@423K@washed.

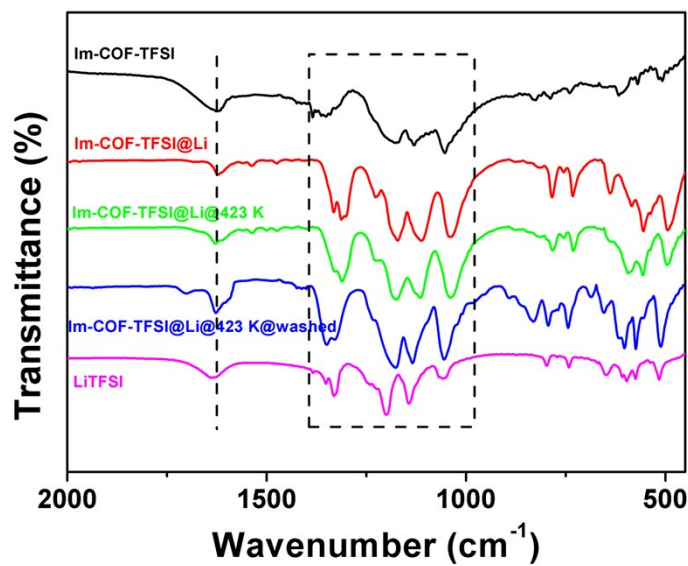


Fig. S21 FT-IR spectra of LiTFSI, Im-COF-TFSI, Im-COF-TFSI@Li, Im-COF-TFSI@Li@423K, and Im-COF-TFSI@Li@423K@washed.

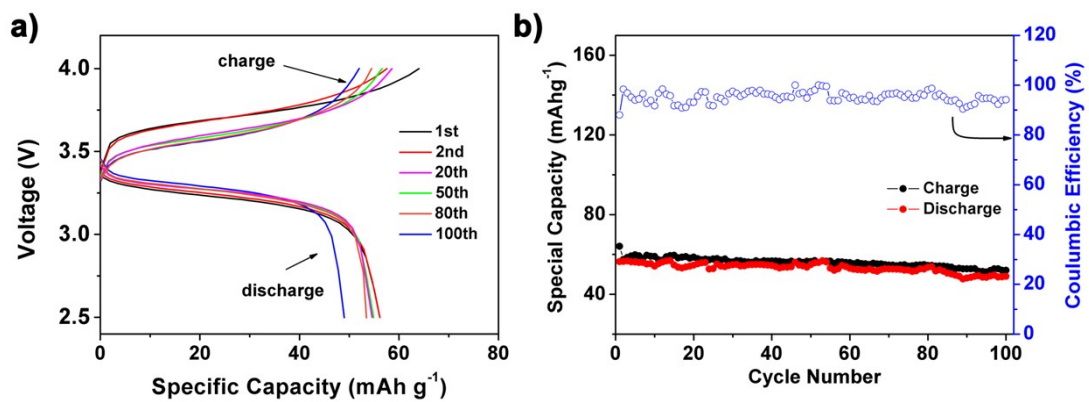


Fig. S22 (a) Charge–discharge curves of Li/Im-COF-TFSI@Li/LiFePO₄ at 0.1 C under room temperature. (b) Cycling performance of the Li/Im-COF-TFSI@Li/LiFePO₄ at 0.1 C under room temperature.

Table S7 Summary of capacities of Li/Im-COF-TFSI@Li/LiFePO₄ and reported COF & MOF-based solid-state Li-ion batteries (LFP = LiFePO₄).

Materials	Capacity (mAh g ⁻¹)	Year	Ref.
Li/PEO+MOF-5+LiTFSI/LFP (all-solid)	143 at 0.2 C (60 °C)	2013	S24
Li/PEO+Mg-BTC-MOF+LiTFSI/LFP (all-solid)	115 at 0.1 C (70 °C)	2014	S25
Li/PEO+Al-BTC-MOF+LiTFSI/LFP (all-solid)	135 at 0.1 C (70 °C)	2014	S5
Li/Li-Ionic liquid+MOF/LFP (solid-like)	145 at 0.5 C (150 °C)	2018	S8
Li/UiO-66-NH ₂ +PEGDA+LiTFSI /LFP (all-solid)	140 at 0.2 C (RT)	2018	S26
Li/Li-IL+MOF+LLZO/LFP (solid-like)	140 at 0.1 C (RT)	2018	S9
Li/P@CMOF/LFP (all-solid)	141 at 0.1 C (60 °C)	2019	S27
Li/ILE@MOF/LFP (solid-like)	151 at 0.1 C (60 °C)	2019	S28
Li/ UIO+Li-IL/LFP (solid-like)	130 at 0.2 C (60 °C)	2019	S11
Li/COF-PEO-9-Li/LFP (all-solid)	120 at 0.02 C (100 °C)	2019	S19
Li/PVDF+H-COF-1@10/LFP (solid-like)	145 at 0.25 C (RT)	2019	S21
Li/Im-COF-TFSI@Li/LFP (all-solid)	123 at 0.1 C (80 °C)	2019	This work

References

- [S1] A. Rit, T. Pape and F. E. Hahn, Self-assembly of molecular cylinders from polycarbene ligands and Ag(I) or Au(I). *J. Am. Chem. Soc.*, 2010, **132**, 4572–4573.
- [S2] R. E. Gawley, H. Mao, M. M. Haque, J. B. Thorne and J. S. Pharr, Visible fluorescence chemosensor for saxitoxin. *J. Org. Chem.*, 2007, **72**, 2187–2191.
- [S3] B. M. Wiers, M. L. Foo, N. P. Balsara and J. R. Long, A solid lithium electrolyte via addition of lithium isopropoxide to a metal–organic framework with open metal sites. *J. Am. Chem. Soc.*, 2011, **133**, 14522–14525.
- [S4] R. Ameloot, M. Aubrey, B. M. Wiers, A. P. Gomora-Figueroa, S. N. Patel, N. P. Balsara and J. R. Long, Ionic conductivity in the metal–organic framework UiO-66 by dehydration and insertion of lithium tert-butoxide. *Chem.–Eur. J.*, 2013, **19**, 5533–5536.
- [S5] C. Gerbaldi, J. R. Nair, M. A. Kulandainathan, R. S. Kumar, C. Ferrara, P. Mustarelli and A. M. Stephan, Innovative high performing metal–organic framework (MOF)-laden nanocomposite polymer electrolytes for all-solid-state lithium batteries. *J. Mater. Chem. A*, 2014, **2**, 9948–9954.
- [S6] S. S. Park, Y. Tulchinsky and M. Dinca, Single-ion Li⁺, Na⁺, and Mg²⁺ solid electrolytes supported by a mesoporous anionic Cu-azolate metal–organic framework. *J. Am. Chem. Soc.*, 2017, **139**, 13260–13263.
- [S7] L. Shen, H. Wu, F. Liu, J. L. Brosmer, G. Shen, X. Wang, J. I. Zink, Q. Xiao, M. Cai, G. Wang, Y. Lu and B. Dunn, Creating lithium-ion electrolytes with biomimetic ionic channels in metal–organic frameworks. *Adv. Mater.*, 2018, **30**, 1707476.

- [S8] Z. Wang, R. Tan, H. Wang, L. Yang, J. Hu, H. Chen and F. Pan, A metal–organic-framework-based electrolyte with nanowetted interfaces for high-energy-density solid-state lithium battery. *Adv. Mater.*, 2018, **30**, 1704436.
- [S9] Z. Wang, Z. Wang, L. Yang, H. Wang, Y. Song, L. Han, K. Yang, J. Hu, H. Chen and F. Pan, Boosting interfacial Li^+ transport with a MOF-based ionic conductor for solid-state batteries. *Nano Energy*, 2018, **49**, 580–587.
- [S10] M. M. Elise, S. P. Sarah and D. Mircea, High Li^+ and Mg^{2+} conductivity in a Cu-azolate metal–organic framework. *J. Am. Chem. Soc.*, 2019, **141**, 4422–4427.
- [S11] J. F. Wu and X. Guo, Nanostructured metal–organic framework (MOF)-derived solid electrolytes realizing fast lithium ion transportation kinetics in solid-state batteries. *Small*, 2019, **15**, 1804413.
- [S12] S. Fischer, J. Roeser, T. C. Lin, R. H. DeBlock, J. Lau, B. S. Dunn, F. Hoffmann, M. Froba, A. Thomas and S. H. Tolbert, A metal–organic framework with tetrahedral aluminate sites as a single-ion Li^+ solid electrolyte. *Angew. Chem. Int. Ed.*, 2019, **57**, 16683–16687.
- [S13] A. Petronico, T. P. Moneypenny, B. G. Nicolau, J. S. Moore, R. G. Nuzzo and A. A. Gewirth, Solid–liquid lithium electrolyte nanocomposites derived from porous molecular cages. *J. Am. Chem. Soc.*, 2018, **140**, 7504–7509.
- [S14] Y. Du, H. Yang, J. M. Whiteley, S. Wan, Y. Jin, S. H. Lee and W. Zhang, Ionic covalent organic frameworks with spiroborate linkage. *Angew. Chem. Int. Ed.*, 2016, **55**, 1737–1741.

- [S15] D. A. Vazquez-Molina, G. S. Mohammad-Pour, C. Lee, M. W. Logan, X. Duan, J. K. Harper and F. J. Uribe-Romo, Mechanically shaped two-dimensional covalent organic frameworks reveal crystallographic alignment and fast Li-ion conductivity. *J. Am. Chem. Soc.*, 2016, **138**, 9767–9770.
- [S16] Y. Zhang, J. Duan, D. Ma, P. Li, S. Li, H. Li, J. Zhou, X. Ma, X. Feng and B. Wang, Three-dimensional anionic cyclodextrin-covalent organic frameworks. *Angew. Chem. Int. Ed.*, 2017, **56**, 16313–16317.
- [S17] H. Chen, H. Tu, C. Hu, Y. Liu, D. Dong, Y. Sun, Y. Dai, S. Wang, H. Qian, Z. Lin and L. Chen, Cationic covalent organic framework nanosheets for fast Li-ion conduction. *J. Am. Chem. Soc.*, 2018, **140**, 896–899.
- [S18] Q. Xu, S. Tao, Q. Jiang and D. Jiang, Ion conduction in polyelectrolyte covalent organic frameworks. *J. Am. Chem. Soc.*, 2018, **140**, 7429–7432.
- [S19] G. Zhang, Y. Hong, Y. Nishiyama, S. Bai, S. Kitagawa and S. Horike, Accumulation of glassy poly(ethylene oxide) anchored in covalent organic framework as solid-state Li⁺ electrolyte. *J. Am. Chem. Soc.*, 2019, **141**, 1227–1234.
- [S20] Z. Guo, Y. Zhang, Y. Dong, J. Li, S. Li, P. Shao, X. Feng and B. Wang, Fast ion transport pathway provided by polyethylene glycol confined in covalent organic frameworks. *J. Am. Chem. Soc.*, 2019, **141**, 1923–1927.
- [S21] D. Dong, H. Zhang, B. Zhou, Y. Sun, H. Zhang, M. Cao, J. Li, H. Zhou, H. Qian, Z. Lin and H. Chen, Porous covalent organic frameworks for high transference number polymer-based electrolytes. *Chem. Commun.*, 2019, **55**, 1458–1461.

- [S22] K. Jeong, S. Park, G. Y. Jung, S. H. Kim, Y.-H. Lee, S. K. Kwak and S. Y. Lee, Solvent-free, single lithium-ion conducting covalent organic frameworks. *J. Am. Chem. Soc.*, 2019, **141**, 5880–5885.
- [S23] Y. Hu, N. Dunlap, S. Wan, S. Lu, S. Huang, I. Sellinger, M. Ortiz, Y. Jin, S. H. Lee and W. Zhang, Crystalline lithium imidazolate covalent organic frameworks with high Li-ion conductivity. *J. Am. Chem. Soc.*, 2019, **141**, 7518–7525.
- [S24] C. Yuan, J. Li, P. Han, Y. Lai, Z. Zhang and J. Liu, Enhanced electrochemical performance of poly(ethylene oxide) based composite polymer electrolyte by incorporation of nano-sized metal–organic framework. *J. Power. Sour.*, 2013, **240**, 653–658.
- [S25] N. Angulakshmi, R. S. Kumar, M. A. Kulandainathan and A. M. Stephan, Composite polymer electrolytes encompassing metal organic frameworks: A new strategy for all-solid-state lithium batteries. *J. Phys. Chem. C*, 2014, **118**, 24240–24247.
- [S26] Z. Zhang, S. Wang, A. Wang, X. Liu, J. Chen, Q. Zeng, L. Zhang, W. Liu and L. Zhang, Covalently linked metal–organic framework (MOF)-polymer all-solid-state electrolyte membranes for room temperature high performance lithium batteries. *J. Mater. Chem. A*, 2018, **6**, 17227–17234.
- [S27] H. Huo, B. Wu, T. Zhang, X. Zheng, L. Ge, T. Xu, X. Guo and X. Sun, Anion-immobilized polymer electrolyte achieved by cationic metal-organic framework filler for dendrite-free solid-state batteries. *Energy Storage Mater.*, 2019, **18**, 59–67.
- [S28] N. Chen, Y. Li, Y. Dai, W. Qu, Y. Xing, Y. Ye, Z. Wen, C. Guo, F. Wu and R.

Chen, A Li⁺ conductive metal organic framework electrolyte boosts the high-temperature performance of dendrite-free lithium batteries. *J. Mater. Chem. A*, **2019**, 7, 9530–9536.